Decellularized Lung Extracellular Matrix Scaffold Promotes Human Embryonic Stem Cell Differentiation towards Alveolar Progenitors

Afshin Noori, D.V.M.[1, 2], Mohammad Reza Mokhber Dezfouli, D.V.M., D.V.Sc.[1, 3], Sarah Rajabi, Ph.D.[2, 4], Fatemeh Ganji, Ph.D.[5], Zahra Ghezelayagh, Ph.D.[2, 6], Elie El Agha, Ph.D.[7], Hossein Baharvand, Ph.D.[2, 6], Sirous Sadeghian Chaleshtori, D.V.M., D.V.Sc.[1, 3*], Yaser Tahamtani, Ph.D.[2, 8*]

1. Department of Internal Medicine, Faculty of Veterinary Medicine, University of Tehran, Tehran, Iran
2. Department of Stem Cells and Developmental Biology, Cell Science Research Center, Royan Institute for Stem Cell Biology and Technology, ACECR, Tehran, Iran
3. Institute of Biomedical Research, University of Tehran, Tehran, Iran
4. Department of Cell Engineering, Cell Science Research Center, Royan Institute for Stem Cell Biology and Technology, ACECR, Tehran, Iran
5. Department of Tissue Engineering and Regenerative Medicine, Faculty of Advanced Technologies in Medicine, Iran University of Medical Sciences, Tehran, Iran
6. Faculty of Sciences and Advanced Technologies in Biology, University of Science and Culture, ACECR, Tehran, Iran
7. Department of Internal Medicine, Universities of Giessen and Marburg Lung Center (UGMLC), Institute for Lung Health (ILH), Cardio-Pulmonary Institute (CPI), Member of the German Center for Lung (DZL), Justus-Liebig University Giessen, Giessen, Germany
8. Reproductive Epidemiology Research Center, Royan Institute for Reproductive Biomedicine, ACECR, Tehran, Iran

Abstract

Objective: Efficient production of functional and mature alveolar epithelial is a major challenge for developing any cell replacement therapy for lung degenerative diseases. The extracellular matrix (ECM) pro-vides a dynamic environment and mediates cellular responses during development and maintenance of tissue functions. The decellularized ECM (dECM) which retains its native-like structure and bio-chemical composition can provide the induction of embryonic stem cell (ESC) differentiation toward the tissue-specific lineages during *in vitro* culture. Therefore, the aim of this study was to evaluate the effect of sheep lung dECM-derived scaffold on differentiation and further maturation of ESC-derived lung progenitor cells.

Materials and Methods: This study was an experimental study. In the first step, a sheep lung was decellularized to achieve dECM scaffolds and hydrogels. Afterwards, the obtained dECM scaffold was evaluated for collagen and glycosaminoglycan contents, DNA quantification, and its ultrastructure. Next, the three experimental groups: i. Sheep lung dECM-derived scaffold, ii. Sheep lung dECM-derived hydrogel, and iii. Fibronectin-coated plates were compared in their abilities to induce further differentiation of human embryonic stem cells (hESCs)-derived definitive endoderm (DE) into lung progenitor cells. The comparison was evaluated by immuno-staining and real-time polymerase chain reaction (PCR) assessments.

Results: We found that the dECM-derived scaffold preserved its composition and native porous structures while lacking nuclei and intact cells. All experimental groups displayed lung progenitor cell differen-tiation as revealed by the RNA and protein expression of NKX2.1, P63 and CK5. DE cells differenti-ated on dECM-derived scaffold and dECM-derived hydrogel showed significant upregulation of *SOX9* gene expression, a marker of the distal airway epithelium. DE cells differentiated on the dECM-derived scaffold compared to the two other groups, showed enhanced expression of *SFTPC* (type 2 alveolar epithelial [AT2] cell marker), *FOXJ1* (ciliated cell marker), and *MUC5A* (secretory cell marker) genes.

Conclusion: Overall, our results suggest that dECM-derived scaffold improves the differentiation of DE cells towards lung alveolar progenitor cells in comparison with dECM-derived hydrogel and fibronectin-coated plates.

Keywords: Decellularization, Differentiation, Hydrogel, Lung, Scaffold

Royan Institute
Cell Journal (Yakhteh)

Introduction

A type 2 alveolar epithelial (AT2)-like progenitor cell differentiation from pluripotent stem cells (PSCs) has been reported using two-dimensional (2D) stepwise differentiation protocols that are initiated by a definitive endoderm (DE) differentiation (1-3). PSCs differentiate to DE cells after activation of the Wnt and TGF-beta signaling pathways by exposure to the CHIR99021 small molecule and the activin A growth factor, respectively (4). Inhibition of TGF/BMP and Wnt signaling pathways in the PSC-derived DE cells provides a generation signal of the anterior foregut endoderm (AFE) cells (5, 6). These cells further differentiate toward the lung progenitor cells and AT2 cells via multiple signaling pathways activation (7).

The native lung extracellular matrix (ECM) contains major biochemical and biophysical properties that provide biocompatibility, elasticity, and porosity requirements supporting cell attachment and fate decision (8, 9). Moreover, physical interaction between cells and the underlying ECM mediates stem cell behaviors such as proliferation, migration, and differentiation (10, 11). It also seems that an instructive memory in the native ECM is able to developmentally determine cell fate and promote tissue-specific differentiation (9). Therefore, using a native lung ECM substrate seems to be ideal for the tissue engineering and likely represents a novel strategy than artificial matrices to mimic the lung ECM scaffold (12, 13). In this regard, a decellularized ECM (dECM) has been generated from various organs, and these dECM scaffolds have been able to be re-cellularized with various cell types (14, 15). Till now, animal decellularized lung scaffolds have been repopulated with primary cells or predifferentiation cells derived from PSCs that demonstrate an efficient generation of mature airway structures in the *in vitro* condition (5, 8). PSC-derived cells are potentially influenced by the ECM and exogenous signals such as paracrine-acting growth factors (16).

Highly conserved ECM components have led to utilize xenogeneic scaffolds in the clinical practice such as heart valve replacement and wound healing therapies (17). An animal source for xenoorgans utilized as decellularized scaffolds that are repopulated with human pluripotent or differentiated cells may resolve the lung donor shortage and facilitate regenerative therapies (13, 17, 18).

It seems that a sheep model may be a proper model for human respiratory diseases, due to similarities in genome (>95% similarity to human), protein structures and growth factors, body weight (50-90 Kg), and pulmonary anatomy and physiology, such as airflow, resistance, compliance, breathing rates, and tidal volumes, which are within the normal ranges present in humans (19, 20). Moreover, it is a cost benefit model because of its availability and low costs (21, 22). In Iran, sheep lung tissues are a by-product of the food industry, so they could easily be obtained as donor tissues for experiments providing opportunities for repeated sampling from different anatomical structures over an extended period (23).

Here, we aimed to elucidate whether a sheep lung dECM-derived scaffold provides crucial cues for the differentiation and further maturation of ESC-derived lung progenitor cells.

Materials and Methods

Ethical approval

In this experimental study, the animal experiments were approved by the Royan Institutional Animal Care and Use Committee, Tehran, Iran (IR.ACECR.ROYAN.REC.1397.271).

Lung decellularization

To minimize potential variation in matrix compounds between samples, only one sheep lung was used, which is a by-product tissue in the food industry in Iran. The superior and inferior cranial lobe pieces with intact small airways and vessels of fresh lung tissues, were promptly delivered to the laboratory and cut into 5×5×1 mm pieces. Lung pieces were rinsed with distilled water (DDW, Inoclon, Iran) for 30 minutes to remove blood cells. Then decellularization of the segments was achieved by 1% sodium deoxycholate (SDC, 302-95-4, Sigma-Aldrich, USA) at 4°C for 24 hours. Lung pieces were then soaked in 1 M NaCl solution (7647-14-5, Sigma-Aldrich, USA) for 1 hour. After the decellularization process was completed, the acellular lung matrix was rinsed with DDW for 48 hours. Finally, samples were soaked in 70% ethanol (64-17-5, Merck, USA) for 10 seconds. To remove ethanol, samples were washed with phosphate buffer saline (PBS, 10010023, Gibco, USA) every 12 hours over a period of 3 days. The procured decellularized lung tissues were stored at -20°C.

Characterization of decellularized lung tissues

Histological staining

Decellularized lung pieces (n=5) were randomly selected and fixed in 4% (w/v) formaldehyde (50-00-0, Sigma-Aldrich, USA) for 4 hours (please add dark/light and temperature condition). Then, the samples were transferred to the tissue processor (DS2080/H, Did Sabz, Iran). Samples were then paraffin (08-7960, Bio-Optica, Italy) embedded and sectioned into 6 μm-slices using a tissue microtome (MicromHM 325, Thermo Scientifc, Germany). The strips were loaded on slides and stained with hematoxylin and eosin (H&E, 15086-94-9, Sigma-Aldrich, USA) to confirm the absence of nuclei. Additionally, staining with 4,6-diamidino-2- phenylindole (DAPI, D8417, Sigma-Aldrich, USA) was carried out on the provided slides. The decellularized lung matrix was evaluated for collagen content by the Masson's trichrome (MT, F7258, Sigma-Aldrich, USA) staining, and for glycosaminoglycan content by Alcian Blue (AB, A5268,

Sigma-Aldrich, USA) and Toluidine blue (T3260, Sigma-Aldrich, USA) staining. Specimens were finally analyzed under the light microscopy (BX51, Olympus) and imaged with an Olympus DP72 digital camera.

DNA quantification

To assess and quantify total DNA content, 30 mg of lyophilized native and decellularized lung tissues (n=3) were treated with digesting buffer solution containing 50 mM Tris-HCl (pH=8, 1185-53-1, Sigma-Aldrich, USA), 50 mM EDTA (60-00-4, Sigma-Aldrich, USA), 10 mM NaCl, and 1% SDS in the presence of 10 µl proteinase K (25530015, Invitrogen, USA) overnight at 65°C in water bath. Samples were purified using phenol-chloroform (136112-00-0, Sigma-Aldrich, USA, 500 µl to each sample) extraction. DNA was precipitated from the upper aqueous layer with 100% ethanol. The extracts were afterwards washed with 70% ethanol (64-17-5, Merck, USA) and dried under laminar hood. After dissolving the resultant pellet in 50 µl DDW, absorbance was measured at 260 nm using a spectrophotometer (Multiskan spectrum, Thermo scientific, Germany) to determine the concentration of DNA.

Scanning electron microscope

Decellularized lung pieces (wight ~ 2 g) were lyophilized using lyophilizer (Alpha 1-2 LD plus, CHRIST, Germany). The pieces were fixed for 24 hours at 4°C in 2.5% glutaraldehyde (G5882, Sigma-Aldrich, USA). After washing with PBS for 2 minutes, (10010023, Gibco, USA) decellularized lung pieces were fixed for 2 hours at 25°C in 1% osmium tetroxide (20816-12-0, Sigma-Aldrich, USA). Then, the pieces were dehydrated in a graded ethanol-water series of 30, 70, 80, 90, and 100% ethanol (64-17-5, Merck, USA) and were left to dry. Finally, the samples were mounted and coated with a thin layer of gold. The electron micrographs were taken at 100x magnification with a scanning electron microscope (VEGA, TESCAN, Czech Republic).

Hydrogel preparation and coating

Decellularized lung pieces were digested with pepsin (9001-75-6, Sigma-Aldrich, USA) at a concentration of 1 mg/mL in 0.1 M HCl (7647-01-0, Merck, USA) and stirred at 4°C for 60 hours. Afterward, the solution was neutralized with 1 M NaOH (1310-73-2, Sigma-Aldrich, USA) at 4°C to induce gelation. After sterilization by UV irradiation, a working concertation of lung ECM hydrogel gel solution was prepared by diluting in Dulbecco's modified Eagle's medium (DMEM, 11320033, Gibco, USA), followed by incubation at 37°C for 5 minutes. To determine the proper hydrogel concentration for cell culture application, 1, 2, 3, and 5 mg/mL hydrogel concentrations were tested. Their impact on the cell growth was analyzed by assessing A549 cell line confluency after 6 days.

Fibronectin coating

Culture plates were positively charged with 50 µg/ mL of poly-L-ornithine (PLO, 27378-49-0, Sigma-Aldrich, USA) to enhance cell attachments and were then incubated at 37°C for 1 hour. After PLO removal, plates were rinsed three times with PBS. Fibronectin (86088-83-7, Sigma-Aldrich, USA) coating at a concentration of 50 µg/ml was applied. Finally, plates were incubated at 37°C for 24 hours.

MTS assay

The 3-(4,5-dimethylthiazol-2-yl)-5-(3-carboxymethoxyphenyl)-2-(4-sulfophenyl)-2H-tetrazolium (MTS) was conducted to examine the efficacy of different coating conditions and analyze their impact on cell proliferation. A549 cells were prepared in the desired concentration (5000 cells per well) and seeded on three different substrates: i. Lung dECM-derived scaffold, ii. Lung dECM-derived hydrogel-coated plates, and iii. fibronectin-coated plates. In addition, A549 cells were cultured in a culture plate as the control group. At day 7, 20 µL of MTS reagent (G1111, Promega Corporation, USA) was added to the plates and then incubated at 37°C for 4 hours in a humidified chamber with 5% CO_2. The absorbance was recorded at a wavelength of 490 nm.

Human embryonic stem cell culture and differentiation

Human embryonic stem cells culturing and preparation

The human embryonic stem cell (hESC) line RH5 (24), obtained from the Royan Stem Cells Bank (Royan Institute, Tehran, Iran), was cultured on the mouse embryonic fibroblasts (MEFs) as a feeder-containing condition. To initiate differentiation, the hESCs were cultured in 6-well Matrigel- (354234, Sigma-Aldrich, USA) coated plates in DMEM/F12 (11320033, Gibco, USA) supplemented with 20% knockout serum replacement (10828010, life technologies, USA), 2 mM l-glutamine (25030081, Gibco, USA), 0.1 mM non-essential amino acids (NEAAs, 11140050, Gibco, USA), 1% insulin-transferrin-selenium (ITS, 41400045, Gibco, USA), 1% penicillin/streptomycin (15070063, Gibco, USA), 0.1 mM β-mercaptoethanol (60-24-2, Sigma-Aldrich, USA), and 100 ng/ml basic fibroblast growth factor (bFGF, Royan Biotech, Iran). The medium was changed every other day. For maintenance, cells were passaged every 6-8 days on the Matrigel (354234, Sigma-Aldrich, USA). For initiating the differentiation protocol, hESCs were singled by trypsin-EDTA (25200056, Gibco, USA) and treated with 10 µM Y27632 (331752-47-7, Sigma-Aldrich, USA) as a ROCK (Rho-associated, coiled-coil containing protein kinase) inhibitor for inhibiting apoptosis. The cells were seeded at a density of 300×10^3 cells/cm² and the differentiation started when the plates reached 80-90% confluency.

Differentiation of human embryonic stem cells towards definitive endoderm cells

After the hESCs reached 80-90% confluency, the

culture medium was changed to DE medium consisting of RPMI 1640 (11875093, Gibco, USA), 1% penicillin/streptomycin, 1% B-27 without vitamin A (12587010, Gibco, USA), and 0.1% bovine serum albumin (BSA, 9048-46-8, Sigma-Aldrich, USA). To achieve mesoendodermal cells, 100 ng/ml activin A (201-069-1, Sigma-Aldrich, USA) and 3 µM CHIR99021 (6-((2-((4-(2,4-dichlorophenyl)-5-(5-methyl-1H-imidazol-2-yl)-2-pyrimidinyl)amino)ethyl)amino)-3-pyridinecarbonitrile), 04-0004-10, Stemgent, USA) a GSK3 inhibitor, were added to the DE medium. After 24 hours, to achieve DE cells, the medium was removed and the cells were treated with fresh DE medium plus 100 ng/ml activin A for three days.

Differentiation of definitive endoderm cells towards anterior foregut endoderm cells

On day 4 of differentiation, colonies were dissociated into single cells using trypsin/EDTA (252000, Gibco, USA). Afterward, DE cells were seeded on three different substrates: i. Lung dECM-derived scaffold (scaffold/24-well plate), ii. 6-well lung ECM-derived hydrogel (hydrogel-coated plate), and iii. 6-well fibronectin-coated plate (86088-83-7, Sigma-Aldrich, USA) (7) (~50,000–75,000 cells/cm). DMEM/F12 containing 1.5 µM Dorsomorphin (04-0024, Stemgent, USA) and 10 µM SB431542 (1614/1, R&D Systems, USA) was added for 24 hours and then for 24 hours, the medium was changed to 10 µM SB431542, a TGF-beta type I receptor inhibitor (13031, Cayman, USA) and 1 µM IWP2 (3533, Tocris, USA).

Differentiation of anterior foregut endoderm cells towards lung progenitor cells

For lung progenitor induction, the achieved anterior foregut endoderm (AFE) was treated with a ventralization cocktail containing 3 µM CHIR99021, 10 ng/mL recombinant human (rh) FGF10 (27, Royan Biotech, Iran), 10 ng/mL rhFGF7 (KG-251, R&D Systems, USA), 10 ng/mL rhBMP4 (BP-314, R&D Systems, USA), 20 ng/mL recombinant murine (rm) EGF (EG-2028, R&D Systems, USA), and 0-1 µM all-trans retinoic acid (ATRA, R2625, Sigma-Aldrich, USA) in differentiation medium for the next 9 days.

For alveolar differentiation, induction process continued at the same culture condition in serum-free conditioned medium containing 3 µM CHIR99021, 10 ng/mL rhFGF10, and 10 ng/mL rhFGF7 for 10 days. The stepwise differentiation protocol which describes the day-dependent addition of small molecules and growth factors shown in Figure S1 (See Supplementary Online Information at www.celljournal.org).

Evaluation of human embryonic stem cells-derived definitive endoderm cells and lung progenitor cells

H&E staining

Histological assessment was carried out for hESC-derived lung progenitor cells on different substrates by H&E staining.

Immunofluorescence and immunochemistry

Slides were rehydrated and antigen retrieval was performed using citrate buffer (pH=6.0, S236984-2, Agilent Technologies, USA) for 20 minutes at 120°C. Afterward, slides and plate of cells were permeabilized and blocked in 0.1% Triton X-100% (2002-93-1, Sigma-Aldrich, USA) and 0.5% BSA (9048-46-8, Sigma-Aldrich, USA) for 1 hour at room temperature. Then, all samples were incubated with primary antibodies against OCT4 (1:200; sc-31984, Santa Cruz, USA), SOX17 (1:200; sc-130295, Santa Cruz, USA), FOXA2 (1:100; AB4125, Sigma-Aldrich, USA), NKX2.1 (1:100; ab227652, Abcam, USA), P63 (1:100; ab110038, Abcam, USA), and pro-SFTPC (1:500; ab40879, Abcam, USA) overnight at 4°C. All samples were then washed three times with PBS, followed by 1 hour of incubation at 37°C with mouse anti-goat FITC (1:400; sc-2356., Santa Cruz, USA), goat anti-mouse FITC (1:400; A11005, Invitrogen, USA), and goat anti-rabbit IgG-TR (1:200; A11037, Invitrogen, USA) secondary antibodies according to the first antibody used. Cell nuclei were stained with DAPI (28718-90-3., Sigma-Aldrich, USA) for 2 minutes.

For immunohistochemistry, the slides were subjected to antigen retrieval and were then immersed in a 0.1% H_2O_2 solution (107209, Sigma-Aldrich, USA) and blocked with 10% goat serum (E-IR-R111, Elabscience, USA) in PBS at 37°C for 1 hour. Afterward, slides were incubated at 4°C overnight with primary antibodies against AQP3 (1:250), CK5 (1:200), P63 (1:200; ab110038, Abcam, USA), and pro-SFTPC (1:400; ab40879, Abcam, USA). On the following day, samples were stained with HRP-conjugated secondary antibody (1:1000; 32260, Thermo Fisher Scientific, Germany) The rinsed sections were incubated with diaminobenzidine for 20 minutes in dark (DAB; Dako, USA). All slides were counterstained with hematoxylin (15 seconds) and washed with running water. Afterwards, sections were mounted and observed using Olympus BX51 microscope.

Flow cytometry

DE cells were dissociated into single cells using trypsin/EDTA (252000, Gibco, USA), for 5 minutes at 37˚C. afterwards the samples were washed with PBS, and collected by centrifugation at 1500 rpm for 5 minutes. Subsequently, dispersed cells were fixed in 4% paraformaldehyde (30525-89-4, Sigma-Aldrich, USA) at 4°C for 20 minutes, permeabilized in 0.2% Triton X-100 (Sigma-Aldrich) and blocked in 5% bovine serum albumin (BSA, 9048-46-8, Sigma-Aldrich, USA) for 45 minutes.
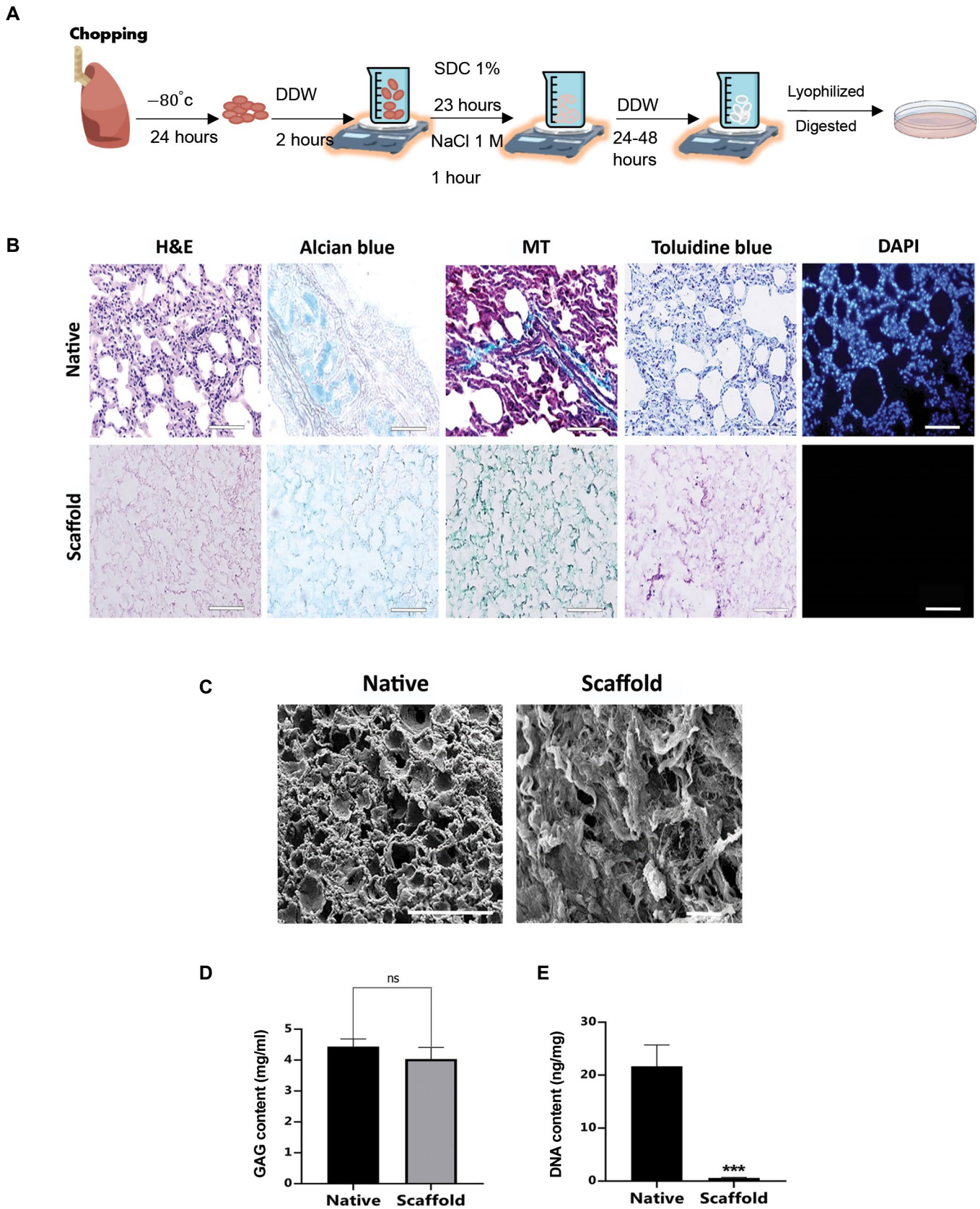
Fig.1: Decellularization procedure, hydrogel formation and characterization. **A.** Schematic representation of lung decellularization procedure and hydrogel formation, **B.** Histological analysis of native sheep lung and decellularized sheep lung ECM-derived scaffold using H&E, Alcian blue, MT, Toluidine blue and DAPI staining (n=3 biological repeats, scale bar: 50 μm), **C.** Representative SEM photomicrographs of native lung (scale bar: 200 μm) and decellularized lung ECM-derived scaffold (scale bar: 50 μm). **D.** Quantification of GAGs content of native and decellularized scaffold (n=4). **E.** DNA quantification assay (n=3). DDW; Double distilled water, SDC; Sodium deoxycholate, PBS; Phosphate buffered saline, MT; Masson's trichrome, SEM; scanning electron microscopy, ECM; Extracellular matrix, GAGs; glycosaminoglycans, h; Hour, ns; Not significant, and ***; P<0.001.
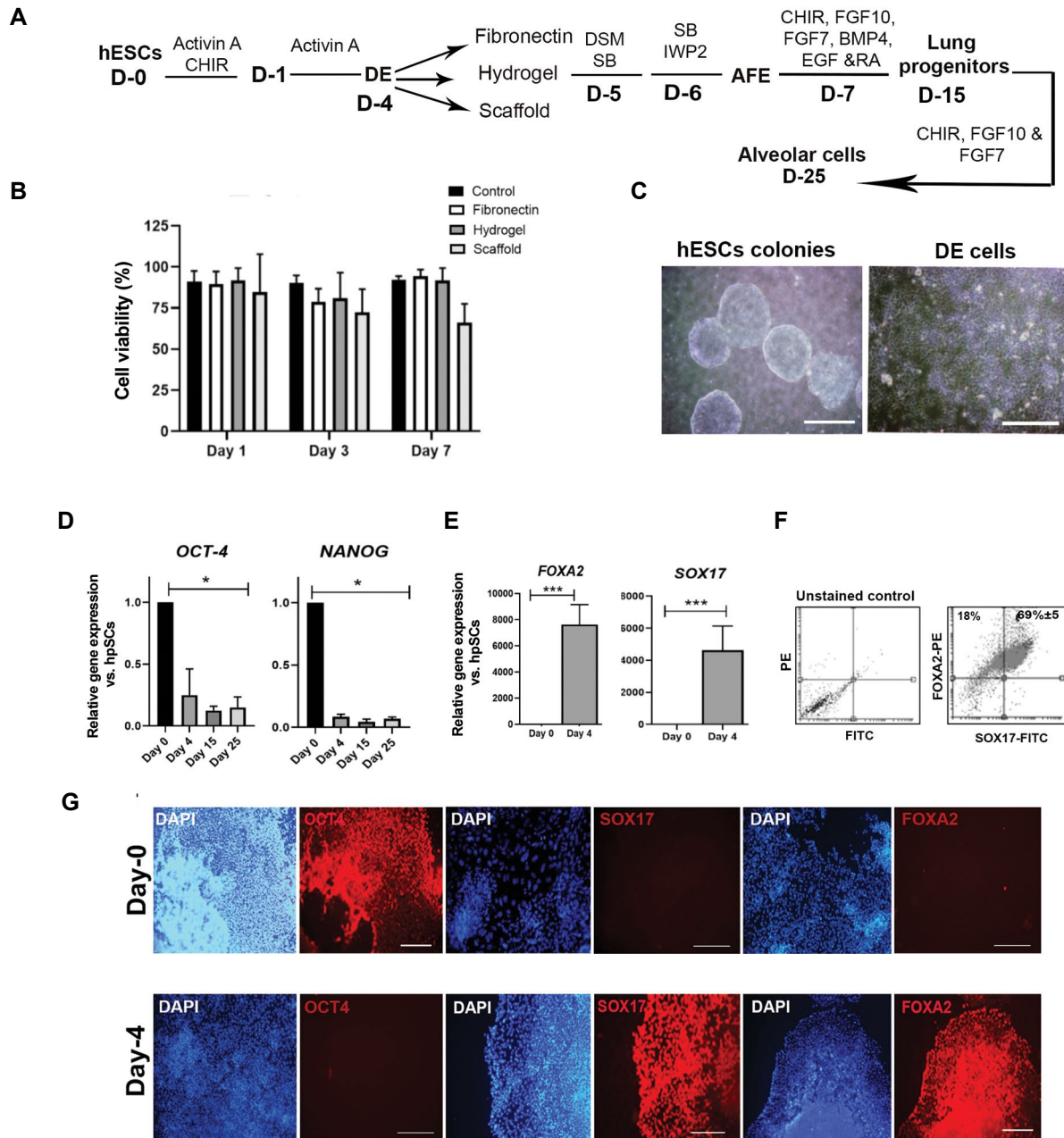
Fig.2: Characterization of hESC-derived definitive endoderm cells at day 4 of differentiation. **A.** Schematic representation of lung differentiation protocol showing differentiation of hESCs into DE cells in the presence of small molecules and growth factors and replating lung progenitors on the different beds including fibronectin, hydrogel, and dECM at day 15. **B.** Determining the cell viability percentage by the MTS assay at days 1, 3, and 7 after the A549 cell line culture on the different beds. A549 cells were cultured as a control group (n=4). **C.** Phase-contrast images of typical hESC colonies (scale bar: 500 μm) and DE cells (scale bar: 200 μm) before replating. **D.** qRT-PCR analysis of hPSCs pluripotent marker genes at days 4, 15, and 25 of lung progenitor differentiation. **E-G.** Characterization of hPSC-derived DE cells before replating on fibronectin: **E.** qRT-PCR analysis for *FOXA2* and *SOX17* genes at day 4 of differentiation (n=3). **F.** Flow cytometrically analysis of FOXA2 and SOX17 positive cells (n=3). **G.** Evaluation of OCT4, FOXA2, and SOX17 protein expression in both hESC (upper panel scale bar: 500 μm, 200 μm, 500 μm, respectively) and DE cells (lower panel: 500 μm) by immunostaining. hESC; Human embryonic stem cell, dECM; Decellularized extracellular matrix, D; Day; DE; Definitive endoderm, AFE; Anterior foregut endoderm, hPSC; Human pluripotent stem cell, qRT-PCR; Quantitative real-time-polymerase chain reaction, *; P<0.005, and ***; P<0.001.

Decellularized lung extracellular matrix and hydrogel coating induce further differentiation of definitive endoderm cells towards lung progenitors and alviolar cells

To assess the impact of lung dECM-derived hydrogel and scaffold on DE further differentiation in comparison with fibronectin-coated plates, hESC-derived DE cells were replated on three different substrates. At day 15 of the lung progenitor differentiation, morphological heterogeneity in fibronectin- (Fig.S3A, See Supplementary Online Information at www.celljournal.org) and hydrogel- (Fig. S3B, See Supplementary Online Information at www. celljournal.org) coated plates was observed. H&E staining of cells differentiated on the scaffold revealed a subset of epithelial cells that lined the lumen (Fig. S3C, See Supplementary Online Information at www. celljournal.org). At day 15 of differentiation, cultured DE cells on the fibronectin expressed NKX2.1, P63, and

FOXA2 proteins (Fig.S3D, See Supplementary Online Information at www.celljournal.org); while DE cells cultured on the hydrogel only expressed NKX2.1 and FOXA2 proteins (Fig.S3E, See Supplementary Online Information at www.celljournal.org).

The morphology of lung progenitor cells on the fibronectin-and hydrogel-coated plates at day 15 of differentiation was shown in Figure 3A, B. Immunostaining revealed that cells expressed NKX2.1 and also pro-surfactant protein C (pro-SFTPC), a marker of AT2 cells, at day 15 of differentiation in both fibronectin-and

hydrogel-coated plates (Fig.3A, B). H&E staining of the dECM revealed that lung progenitor cells were located in alveolar structures, particularly in thin alveolar walls. In line with these findings, SEM micrographs showed that the scaffold surface was densely covered by differentiated cells. Differentiated cells on the dECM were analyzed for the expression of basal and AT2 cell markers at day 15 of differentiation. Markers of basal cells, CK5 and P63 proteins, were detected in airways lining cells and also, AT2 markers, SFTPC and AQP3 proteins, were observed in the alveolar regions (Fig.3C).
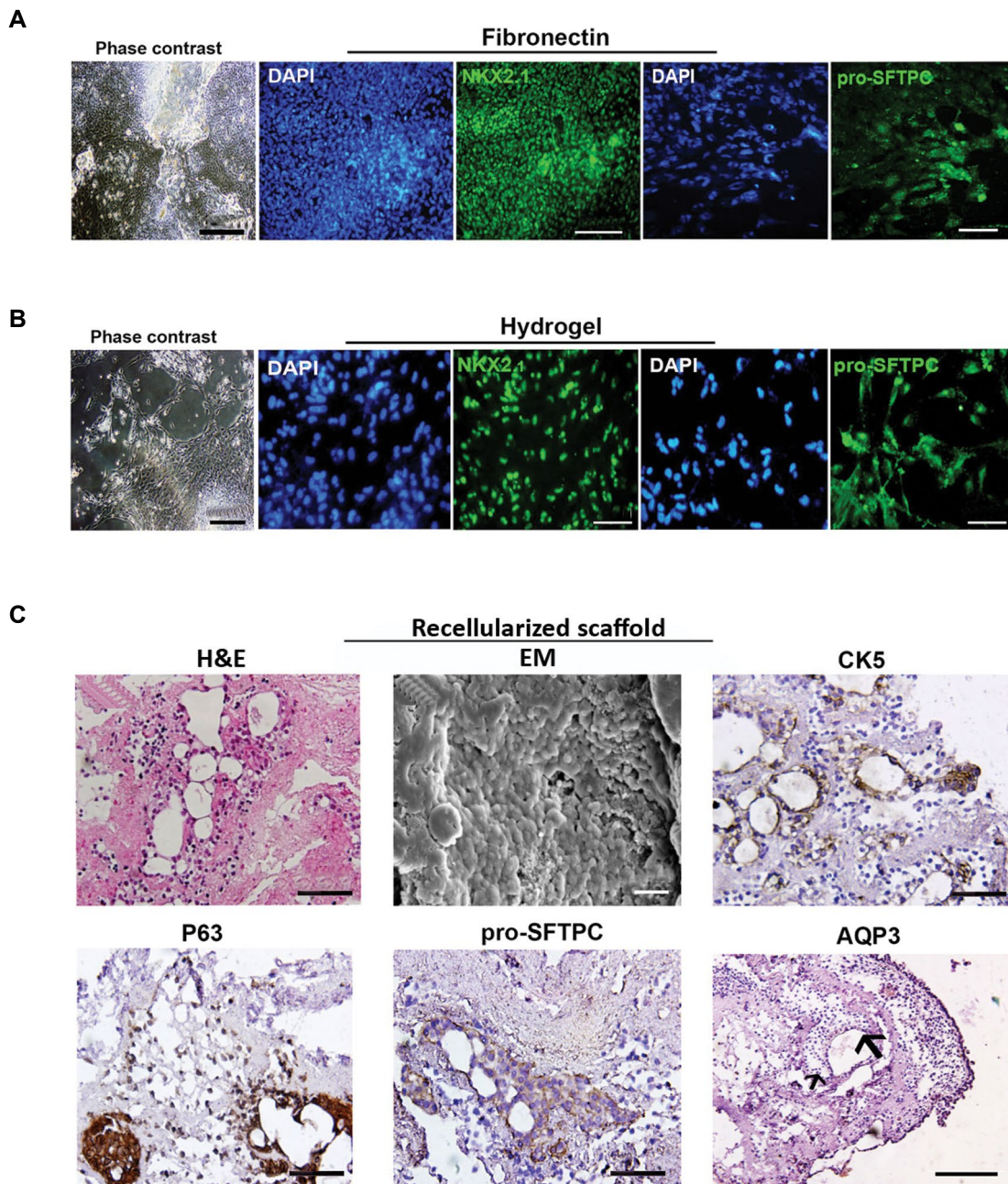

Fig.3: Morphology and phenotypical characterization of hESC-derived lung progenitor cells at day 25 of differentiation. Phase-contrast images of cells and immunostaining for NKX2.1 and pro-surfactant protein C (pro-SFTPC) proteins in lung progenitors differentiated on **A.** Fibronectin (scale bar: 200 μm, 100 μm, 50 μm, respectively) and **B.** Hydrogel-coated plates (scale bar: 100 μm, 50 μm, 50 μm, respectively). **C.** H&E staining shows the attachment and retention of differentiated cells at day 25 (scale bar: 50 μm) and SEM photomicrograph shows the recellularization of scaffold surface reseeded with 15-day-old progenitor cells (scale bar: 20 μm). Immunohistochemistry for CK5, P63, pro-SFTPC, and AQP3 protein markers in the cells that were grown on the dECM scaffold at day 25 (scale bar: 50 μm, 50 μm, 50 μm, and 100 μm respectively). HESCs; Human embryonic stem cells and dECM; Decellularized extracellular matrix.

Gene expression analysis revealed a significant upregulation level of the DE marker, *FOXA2* gene, in the cells cultured on fibronectin (P<0.0001) in comparison with other groups at days 15 and 25 of differentiation (Fig.4). Moreover, cells differentiated on the hydrogel showed a significant upregulation level of *FOXA2* gene (P<0.01) in comparison with differentiated cells on the scaffold at day 25 of differentiation. The RNA expression level of *SOX9* as a distinct marker in distal airways and developing the alveolar region showed a significant increase in hydrogel (P<0.01) and dECM (P<0.05) groups in comparison with the fibronectin group at day 25 of

differentiation. Interestingly, cells seeded on the scaffold showed a significant upregulation level of *SFTPC* RNA expression (P<0.0001) in comparison with other groups. Markers of differentiated airway epithelium including *FOXJ1* (ciliated cells) and *MUC5A* (secretory cells) mRNA expression demonstrated obvious upregulation in cells differentiated on the scaffold at day 25 of differentiation (P<0.001 and P<0.0001, respectively). In addition, RNA expression levels of basal cell markers including *CK5* and *P63* were significantly upregulated in the scaffold group at day 25 of differentiation (P<0.0001).
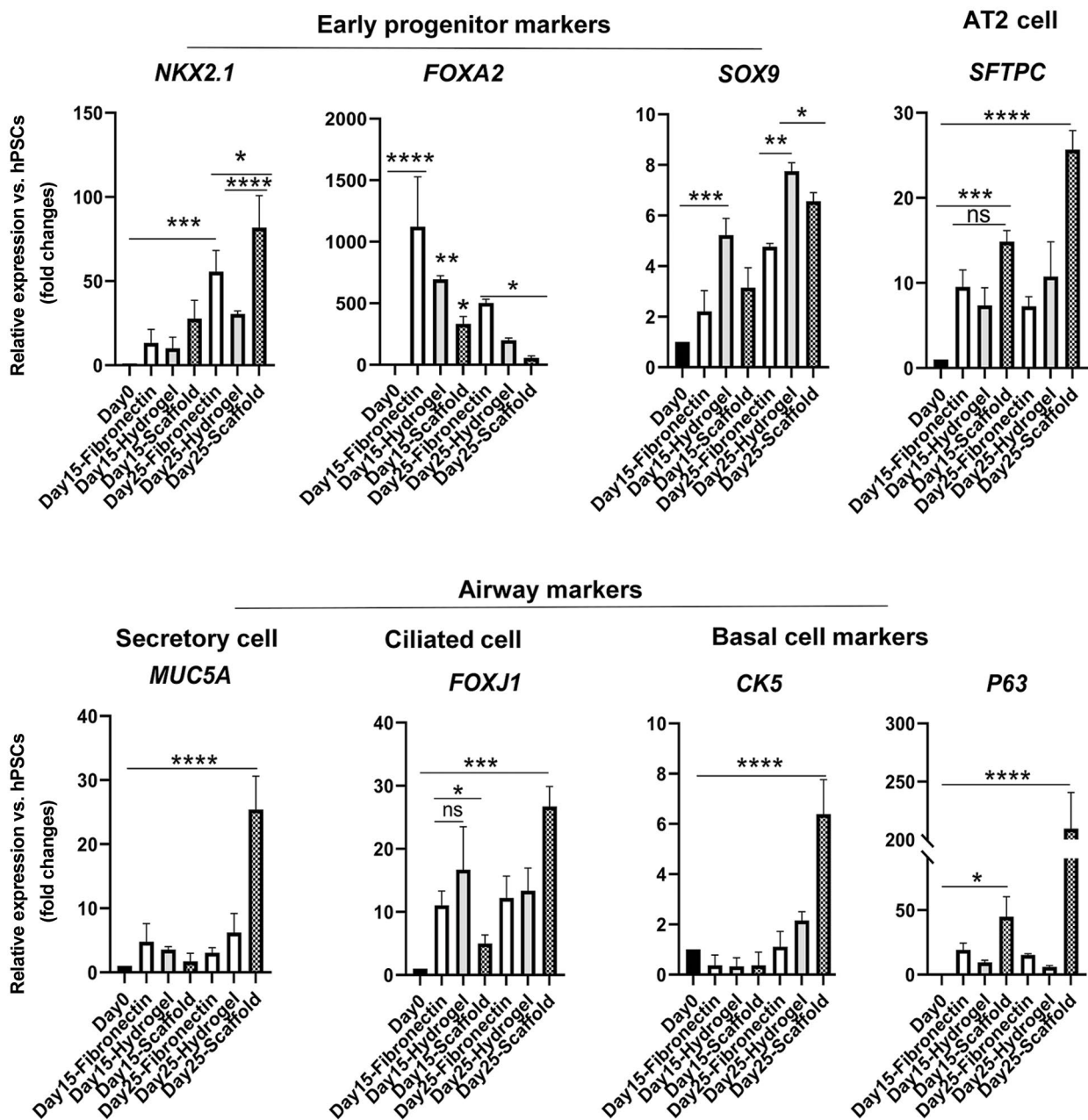

Fig.4: Quantitative RT-PCR analysis at days 0, 15, and 25 of differentiation. Quantitative RT-PCR analysis was conducted for undifferentiated hESCs and day 15 and 25 of differentiated cells. The expression level of the target gene was normalized to *GAPDH* and presented relative to hESC. Data are presented as mean ± SD. Significant difference was identified using the t test with unequal variance (n=3). RT-PCR; Real-time-polymerase chain reaction, hESCS; Human embryonic stem cells, ns; Not significant, *; P<0.05, **; P<0.01, ***; P<0.001, and ****; P<0.0001.

Discussion

Due to the complex interactions between cells and extracellular matrices during lung development, *in vitro* differentiation of a PSC into the functional airway and alveolar epithelial cells is a current challenge. The present study examined the impact of the decellularized sheep lung scaffold and hydrogel on the lung progenitor cell differentiation from hESCs derived DE cells. We observed that the native lung ECM structure enhances *in vitro* differentiation of type 2 alveolar epithelial (AT2) and subsequently induces *AQP3* and *SFTPC* RNA expression levels. We also evaluated the RNA expressing levels of distal airway stem/progenitor cell markers.

Accordingly, it has been shown that proximal airway development using acellular lung tissues along with the differentiation of PSCs into mature airway epithelial cells including ciliated cells, club cells, and basal cells morphologically and functionally resemble the native airways (9). It has been shown that matrix topography regulates stem cell differentiation by changing cell shape through a contact guidance process (17). In 3D structures of normal tissues the collagen fibers of the ECM, arrange parallel to the epithelium, that influence cellular proliferation and differentiation, particularly during embryonic development (26). The topographic features of the ECM may induce a focal adhesion formation triggering intracellular signal transduction (27) which induces an architecture deformation and alteration of gene expression profiles (28).

Our immunostaining experiments revealed that hESC-derived pro-SFTPC-, CK5-, and P63- expressing cells were able to repopulate decellularized alveolar structures of the scaffold in culture providing their regenerative potential, as was also reported by Ghaedi et al. (5). Repopulation of the scaffold by hESC-derived cells highlights the importance of 3D ECM topographic characteristics in supporting cell adherence and maturation (9). Lung heterogeneous cell populations are detectable by various molecular markers including basal cells (CK5 and P63), ciliated cells (FOXJ1), secretory cells (MUC5A) throughout all part of bronchiolar airways, distal or peripheral progenitors (NKX2.1 /SOX9), and AT2 cells (SFTPC) (29). According to our gene expression analysis, decellularized sheep lung scaffolds successfully induced the differentiation of an AFE cells into all mentioned lung cell populations on the 25-day duration. Moreover, our data suggest that hESC-derived progenitors may possess bi-potent differentiation capabilities at day 15 of differentiation that allows them to give rise to both distal airway and alveolar epithelial cells as reported in human embryonic lung epithelial multipotent progenitor cells (30). After recellularization of lung dECM with day 15 differentiated progenitor cells, the bronchiolar airway epithelial cell-associated genes, *FOXJ1* and *MUC5A*, showed a significant upregulation. The upregulation of these genes was also observed by Shojaie et al. (9).

Natural hydrogels have been extensively generated from various decellularized tissues (31, 32), as well as lung-derived tissues (33). Detergent-based decellularization and enzymatic solubilization of lung tissue methods have been widely used for lung ECM hydrogel preparation (34-36). In contrast to decellularized lung scaffolds as a 3D culture system, 2D monolayer culture on the hydrogel were used to induce the transition from PSCs into pro-SFTPC-expressing cells. Such a method led to the production of typical epithelial cell colonies in a 2D culture. Although, ECM-derived hydrogels preserve the stiffness and viscoelasticity of the intact lung, monolayer cultures do not resemble the lung microenvironment nor mimic the native ECM features (26). In addition, the procedure used to prepare an ECM-derived hydrogel has drawbacks including disruption of proteoglycans and ECM-bound growth factors that are needed for proper cell behaviors (37, 38).

To overcome donor shortage in organ transplantation and explore potential therapeutic options for organ failure, xenogeneic decellularized lung scaffolds have been recellularized with human cells and re-implanted into animal recipients (39). Moreover, vascular networks and airways were repopulated by human umbilical vein endothelial cells and basal cells, respectively. However, these challenges may be at least partially overcome by extensive preclinical studies using large animal models to achieve a valid clinical-grade procedure for translating the technology into a robust therapy (40).

Conclusion

Our results revealed a better AT2 differentiation, when hESCs were cultured on the decellularized sheep lung ECM-derived scaffolds in comparison with the decellularized sheep lung ECM-derived hydrogel or usual fibronectin. We found that the 3D culture of ESC-derived lung progenitors on the lung ECM-derived scaffolds resulted in a significant upregulation RNA level of AT2 markers.

Acknowledgments

Authors' Contributions

M.R.M.D., S.S.Ch., E.E.A., Y.T., H.B., S.R.; Designed the study and the experiments. A.N., Z.Gh.; Performed the experiments. A.N., F.G., Z.Gh.; Analyzed the data.

References

1. Mitchell A, Drinnan CT, Jensen T, Finck C. Production of high purity alveolar-like cells from iPSCs through depletion of uncommitted cells after AFE induction. Differentiation. 2017; 96: 62-69.

2. Jacob A, Morley M, Hawkins F, McCauley KB, Jean J, Heins H, et al. Differentiation of human pluripotent stem cells into functional lung alveolar epithelial cells. Cell Stem Cell. 2017; 21(4): 472-488. e10.

3. van Riet S, Ninaber DK, Mikkers HMM, Tetley TD, Jost CR, Mulder AA, et al. In vitro modelling of alveolar repair at the air-liquid interface using alveolar epithelial cells derived from human induced pluripotent stem cells. Sci Rep. 2020; 10(1): 5499.

4. Rodrigues Toste de Carvalho AL, Liu HY, Chen YW, Porotto M, Moscona A, Snoeck HW. The in vitro multilineage differentiation and maturation of lung and airway cells from human pluripotent stem cell-derived lung progenitors in 3D. Nat Protoc. 2021; 16(4): 1802-1829.

5. Ghaedi M, Calle EA, Mendez JJ, Gard AL, Balestrini J, Booth A, et al. Human iPS cell-derived alveolar epithelium repopulates lung extracellular matrix. J Clin Invest. 2013; 123(11): 4950-4962.

6. Ikeo S, Yamamoto Y, Ikeda K, Sone N, Korogi Y, Tomiyama L, et al. Core-shell hydrogel microfiber-expanded pluripotent stem cell-derived lung progenitors applicable to lung reconstruction in vivo. Biomaterials. 2021; 276: 121031.

7. Huang SX, Islam MN, O'Neill J, Hu Z, Yang YG, Chen YW, et al. Efficient generation of lung and airway epithelial cells from human pluripotent stem cells. Nat Biotechnol. 2014; 32(1): 84-91.

8. Gilpin SE, Ren X, Okamoto T, Guyette JP, Mou H, Rajagopal J, et al. Enhanced lung epithelial specification of human induced pluripotent stem cells on decellularized lung matrix. Ann Thorac Surg. 2014; 98(5): 1721-1729; discussion 1729.

9. Shojaie S, Ermini L, Ackerley C, Wang J, Chin S, Yeganeh B, et al. Acellular lung scaffolds direct differentiation of endoderm to functional airway epithelial cells: requirement of matrix-bound HS proteoglycans. Stem Cell Reports. 2015; 4(3): 419-430.

10. Burgstaller G, Oehrle B, Gerckens M, White ES, Schiller HB, Eickelberg O. The instructive extracellular matrix of the lung: basic composition and alterations in chronic lung disease. Eur Respir J. 2017; 50(1): 1601805.

11. Mohgan R, Candasamy M, Mayuren J, Singh SK, Gupta G, Dua K, et al. Emerging paradigms in bioengineering the lungs. Bioengineering (Basel). 2022; 9(5): 195.

12. Ashtiani MK, Zandi M, Barzin J, Tahamtani Y, Ghanian MH, Moradmand A, et al. Substrate-mediated commitment of human embryonic stem cells for hepatic differentiation. J Biomed Mater Res A. 2016; 104(11): 2861-2872.

13. Nicolas J, Magli S, Rabbachin L, Sampaolesi S, Nicotra F, Russo L. 3D extracellular matrix mimics: fundamental concepts and role of materials chemistry to influence stem cell fate. Biomacromolecules. 2020; 21(6): 1968-1994.

14. Takasato M, Little MH. Making a kidney organoid using the directed differentiation of human pluripotent stem cells. Methods Mol Biol. 2017; 1597: 195-206.

15. Neishabouri A, Soltani Khaboushan A, Daghigh F, Kajbafzadeh AM, Majidi Zolbin M. Decellularization in tissue engineering and regenerative medicine: evaluation, modification, and application methods. Front Bioeng Biotechnol. 2022; 10: 805299.

16. Ullah I, Busch JF, Rabien A, Ergün B, Stamm C, Knosalla C, et al. Adult tissue extracellular matrix determines tissue specification of human iPSC-derived embryonic stage mesodermal precursor cells. Adv Sci (Weinh). 2020; 7(5): 1901198.

17. Urbanczyk M, Layland SL, Schenke-Layland K. The role of extracellular matrix in biomechanics and its impact on bioengineering of cells and 3D tissues. Matrix Biol. 2020; 85-86: 1-14.

18. Stahl EC, Bonvillain RW, Skillen CD, Burger BL, Hara H, Lee W, et al. Evaluation of the host immune response to decellularized lung scaffolds derived from α-Gal knockout pigs in a non-human primate model. Biomaterials. 2018; 187: 93-104.

19. Viscasillas J, Alonso-Iñigo JM, Gutierrez-Bautista A, Casañ Pallardó M, Redondo JI. Description of ovine model for testing ventilator prototypes in the COVID-19 pandemic. Rev Esp Anestesiol

20. Al Abri R, Kolethekkat AA, Kelleher MO, Myles LM, Glasby MA. Effect of locally administered ciliary neurotrophic factor on the survival of transected and repaired adult sheep facial nerve. Oman Med J. 2014; 29(3): 208-213.

21. Padma AM, Carrière L, Krokström Karlsson F, Sehic E, Bandstein S, Tiemann TT, et al. Towards a bioengineered uterus: bioactive sheep uterus scaffolds are effectively recellularized by enzymatic preconditioning. NPJ Regen Med. 2021; 6(1): 26.

22. Ranaei V, Pilevar Z, Esfandiari C, Khaneghah AM, Dhakal R, Vargas-Bello-Pérez E, et al. Meat value chain losses in Iran. Food Sci Anim Resour. 2021; 41(1): 16-33.

23. Rajabi S, Pahlavan S, Ashtiani MK, Ansari H, Abbasalizadeh S, Sayahpour FA, et al. Human embryonic stem cell-derived cardiovascular progenitor cells efficiently colonize in bFGF-tethered natural matrix to construct contracting humanized rat hearts. Biomaterials. 2018; 154: 99-112.

24. Baharvand H, Ashtiani SK, Taee A, Massumi M, Valojerdi MR, Yazdi PE, et al. Generation of new human embryonic stem cell lines with diploid and triploid karyotypes. Dev Growth Differ. 2006; 48(2): 117-128.

25. Mokhber Dezfouli MR, Sadeghian Chaleshtori S, Moradmand A, Basiri M, Baharvand H, Tahamtani Y. Hydrocortisone promotes differentiation of mouse embryonic stem cell-derived definitive endoderm toward lung alveolar epithelial cells. Cell J. 2019; 20(4): 469-476.

26. de Hilster RHJ, Sharma PK, Jonker MR, White ES, Gercama EA, Roobeek M, et al. Human lung extracellular matrix hydrogels resemble the stiffness and viscoelasticity of native lung tissue. Am J Physiol Lung Cell Mol Physiol. 2020; 318(4): L698-L704.

27. Bandzerewicz A, Gadomska-Gajadhur A. Into the tissues: extracellular matrix and its artificial substitutes: cell signalling mechanisms. Cells. 2022; 11(5): 914.

28. Yang L, Ge L, van Rijn P. Synergistic effect of cell-derived extracellular matrices and topography on osteogenesis of mesenchymal stem cells. ACS Appl Mater Interfaces. 2020; 12(23): 25591-25603.

29. Swarr DT, Wert SE, Whitsett JA. Molecular determinants of lung morphogenesis. Kendig's disorders of the respiratory tract in children. 9th ed. Elsevier; 2019: 26-39. e4.

30. Nikolić MZ, Caritg O, Jeng Q, Johnson JA, Sun D, Howell KJ, et al. Human embryonic lung epithelial tips are multipotent progenitors that can be expanded in vitro as long-term self-renewing organoids. Elife. 2017; 6: e26575.

31. Loneker AE, Faulk DM, Hussey GS, D'Amore A, Badylak SF. Solubilized liver extracellular matrix maintains primary rat hepatocyte phenotype in-vitro. J Biomed Mater Res A. 2016; 104(4): 957-965.

32. Kort-Mascort J, Flores-Torres S, Peza-Chavez O, Jang JH, Pardo LA, Tran SD, et al. Decellularized ECM hydrogels: prior use considerations, applications, and opportunities in tissue engineering and biofabrication. Biomater Sci. 2023; 11(2): 400-431.

33. Pouliot RA, Link PA, Mikhaiel NS, Schneck MB, Valentine MS, Kamga Gninzeko FJ, et al. Development and characterization of a naturally derived lung extracellular matrix hydrogel. J Biomed Mater Res A. 2016; 104(8): 1922-1935.

34. Tebyanian H, Karami A, Motavallian E, Samadikuchaksaraei A, Arjmand B, Nourani MR. Rat lung decellularization using chemical detergents for lung tissue engineering. Biotech Histochem. 2019; 94(3): 214-222.

35. Kuşoğlu A, Yangın K, Özkan SN, Sarıca S, Örnek D, Solcan N, et al. Different decellularization methods in bovine lung tissue reveals distinct biochemical composition, stiffness, and viscoelasticity in reconstituted hydrogels. ACS Appl Bio Mater. 2023; 6(2): 793-805.

36. Li Y, Wu Q, Li L, Chen F, Bao J, Li W. Decellularization of porcine whole lung to obtain a clinical-scale bioengineered scaffold. J Biomed Mater Res A. 2021; 109(9): 1623-1632.

37. Crapo PM, Gilbert TW, Badylak SF. An overview of tissue and whole organ decellularization processes. Biomaterials. 2011; 32(12): 3233-3243.

38. Mendoza-Novelo B, Avila EE, Cauich-Rodríguez JV, Jorge-Herrero E, Rojo FJ, Guinea GV, et al. Decellularization of pericardial tissue and its impact on tensile viscoelasticity and glycosaminoglycan content. Acta Biomater. 2011; 7(3): 1241-1248.

39. Zhou H, Kitano K, Ren X, Rajab TK, Wu M, Gilpin SE, et al. Bioengineering human lung grafts on porcine matrix. Ann Surg. 2018; 267(3): 590-598.

40. Wiles K, Fishman JM, De Coppi P, Birchall MA. The host immune response to tissue-engineered organs: current problems and future directions. Tissue Eng Part B Rev. 2016; 22(3): 208-219.

Reanim (Engl Ed). 2021; 68(10): 592-596.